Published in final edited form as:
Vis Neurosci. 2008 ; 25(1): 95–102. doi:10.1017/S095252380808005X.

HCN4-like Immunoreactivity in Rat Retinal Ganglion Cells

Hanako Oi[1], **Gloria J. Partida**[1], **Sherwin C. Lee**[1], and **Andrew T. Ishida**[1,2]

[1]Section of Neurobiology, Physiology and Behavior, University of California, Davis, California 95616

[2]Department of Ophthalmology and Vision Science, University of California, Davis, California 95616

Abstract

Antisera directed against hyperpolarization-activated, cyclic nucleotide–sensitive ("HCN") channels bind to somata in the ganglion cell layer of rat and rabbit retinas, and mRNA for different HCN channel isoforms has been detected in the ganglion cell layer of mouse retina. However, previous studies neither provided evidence that any of the somata are ganglion cells (as opposed to displaced amacrine cells) nor quantified these cells. We therefore tested whether isoform-specific anti-HCN channel antisera bind to ganglion cells labeled by retrograde transport of fluorophore-coupled dextran. In flat-mounted adult rat retinas, the number of dextran-backfilled ganglion cells agreed with cell densities reported in previous studies, and anti-HCN4 antisera bound to the somata of approximately 40% of these cells. The diameter of these somata ranged from 7 to 30 μm. Consistent with localization to cell membranes, the immunoreactivity formed a thin line that circumscribed individual somata. Optic fiber layer axon fascicles, and the proximal dendrites of some ganglion cells, also displayed binding of anti-HCN4 antisera. These results suggest that the response of some mammalian retinal ganglion cells to hyperpolarization may be modulated by changes in intracellular cAMP levels, and could thus be more complex than expected from previous voltage and current recordings.

Keywords

immunocytochemistry; retinal ganglion cells; HCN channels

Introduction

The voltage sensitivities and gating kinetics of roughly one dozen non-synaptic ion conductances have been assessed by current recordings from dissociated retinal ganglion cells (e.g., Lipton and Tauck, 1987; Lukasiewicz and Werblin, 1988; Tabata and Ishida, 1996; Kim and Rieke 2001; Lee et al., 2003; Hayashida and Ishida 2004). These measurements indicate that spiking in retinal ganglion cells is not simply triggered by depolarization, but that it is also influenced by the subthreshold and suprathreshold membrane potentials traversed, and the time spent at these voltages. Recent molecular and immunostaining methods have detected an even wider variety of ion channels, suggesting that spike generation in ganglion cells may be more complex than previously thought. For example, although hyperpolarization can activate the mixed-cation current known as I_h in rat and goldfish retinal ganglion cells, and although cell-specific differences or pharmacologically-induced changes in I_h have not been described (Eng et al., 1990; Tabata

Address for Correspondence: Andrew Ishida, Section of Neurobiology, Physiology and Behavior, University of California, One Shields Avenue, Davis, California 95616-8519, atishida@ucdavis.edu, telephone and fax: (530) 752-3569.

and Ishida, 1996; Lee and Ishida, 2007), RNA probes for more than one hyperpolarization-activated and cyclic nucleotide–sensitive ("HCN") channel isoform bind to the ganglion cell layer of mouse retina (Moosmang et al., 2001; see also Koizumi et al., 2004), and immunoreactivity for HCN channel isoforms can be seen in some somata within the ganglion cell layer of rat and rabbit retina (Müller et al., 2003; Kim et al., 2003). However, none of these somata were shown to belong to ganglion cells rather than displaced amacrine cells, and properties such as cell numbers, cell body size distributions, and regional distributions can not be determined from the images published to date. Here, we report these characteristics based on adult rat retinal ganglion cells that have bound antisera against mammalian HCN channel isoforms (Santoro and Tibbs, 1999) in flat-mounted retinas after retrograde labeling via the optic nerve.

Materials and Methods

Animals

Long-Evans rats (female; P60–P120; 150–250 g) were obtained from Harlan Bioproducts (San Diego, CA) and housed in standard cages at ~23 °C on a 12-hr/12-hr light/dark cycle. All animal care and experimental protocols were approved by the Animal Use and Care Administrative Advisory Committee of the University of California, Davis.

Protein isolation and western blot analysis

Protein was isolated as described elsewhere (Partida et al., 2004), with the following modifications to study membrane fraction proteins. After centrifuging the homogenate from twenty retinas at 13000 × g for 15 min at 4 °C, the supernatant was collected and the pellet resuspended in homogenization buffer. This buffer contained protease inhibitors and was supplemented with phosphatase inhibitors [50 mM NaF, 50 mM β glycerol phosphate (pH 8.0), and 0.2 mM Na orthovanadate; see below for sources of chemicals]. After centrifuging, resuspending the pellet, and centrifuging again, the supernatants from all three spins were pooled and centrifuged at 45000 × g for 1 hr at 4 °C. The resulting pellet was resuspended in 500 μl of homogenization buffer, assayed by the Bradford method for total protein, and denatured by mixing with NuPage LDS sample buffer (4x) and NuPage Reducing agent (10x) and heating to 70 °C for 10 min. Aliquots were loaded at 50–100 μg of protein per lane onto a 10% bis-tris polyacrylamide gradient gel (NuPage) and run with MOPS running buffer. Protein standards (Benchmark and See Blue) were run in lanes adjacent to the samples.

Proteins were transferred to nitrocellulose membranes and probed with antisera as described previously (Partida et al., 2004). Membranes were incubated either in an anti-HCN4 antibody or anti-HCN4 antibody pre-adsorbed with a two-fold higher concentration of control antigen (see the "Antibodies" section below for details), rinsed in TBST, and incubated in secondary antibody conjugated to horseradish peroxidase. Primary antibody and antigen-blocked antibody were diluted 1:1000, while secondary antibody was diluted 1:5000, all in TBST containing 3% BSA (w/v). Protein bands were visualized using ECL detection with SuperSignal West Pico Chemiluminescent Substrate.

Retrograde labeling

Rats were anesthetized with intraperitoneally injected sodium pentobarbital (25 mg/kg). The conjunctiva was cut and the globe retracted with forceps to expose the optic nerve. After nicking the optic nerve with scissors, approximately 2 mg of fixable 10-kD dextran coupled to Alexa Fluor 568 was deposited against the retinal end of the cut optic nerve fibers. Each rat was allowed to survive 23 to 28 hr to allow the retrograde marker to reach the retina.

Flat mounts

Rats were administered a lethal dose of sodium pentobarbital (150 mg/kg, IP). Retinas were fixed by cardiac perfusion of 4% paraformaldehyde in phosphate-buffered saline (PBS; pH 7.4) following preperfusion of oxygenated Hank's balanced salt solution. After each eye was enucleated and hemisected, the lens was removed, and the posterior "eyecup" placed in a mixture of ~0.2% picric acid and 2% paraformaldehyde in PBS (pH 7.4) overnight at 4 °C. After rinsing in PBS, the retinas were isolated, placed vitreous side up on a nitrocellulose filter disc, and cut radially by a few mm from the retinal periphery toward the optic nerve head. The filter and retina were placed on a Swinnex adapter (Millipore; Billerica, MA) and suction was applied to the opposite side while PBS was dropped over the retina. When the retina was firmly attached, the vitreous was removed with filter paper, and a scalpel was used to reduce the thickness of the flat mounts by slicing the inner retina off of the outer retina. Some of these retinas were cut into pieces for subsequent comparisons (e.g., test tissue vs. negative control). These preparations were then washed with PBS; incubated for 20–30 min in a saturated solution of Li_2CO_3 in PBS to extract picric acid; rinsed with PBS; incubated in 0.1 M citric acid (pH 6.0) at 85 °C for 30 min; quenched in glycine (1% in PBS) for 1 hr at room temperature; permeabilized with Triton X-100 (0.05% in PBS) for 30 min at room temperature; blocked with Image-iT for 3.5 hrs at room temperature; incubated in primary antibody for 3.5 days at 4 °C; rinsed with PBS; and incubated in secondary antibody for 2.5 hrs at room temperature. After a final rinse, the retinas were placed ganglion-cell-side up on Superfrost/Plus slides, and covered with FluorSave and a #1.5 glass coverslip.

Imaging

Confocal images were obtained by excitation of the fluorescent dyes conjugated to the secondary antibodies and introduced dextran. Images were acquired on an Olympus FluoView 300 Confocal System (version 4.3) interfaced to an Olympus IX70 inverted microscope. Excitation was provided by Ar (488 nm) and Kr (568 nm) lasers. Analysis was restricted to the ganglion cell and optic fiber layers, where data were collected in series of optical sections at 0.7-to 1-μm intervals, with 2- or 3-frame Kalman averaging for each section. When acquiring images of different fluorophores, we excited both fluorophores simultaneously, collected the fluorescence from both fluorophores at the same time through parallel filter sets, and adjusted the detector settings for each dye to minimize any signal arising from the other dye. Images due to each dye were separated and cropped, and changes in color space were applied as needed using the public domain program ImageJ (version 1.37, available on the Internet at http://rsb.info.nih.gov/ij/). Any subsequent adjustments to brightness or contrast were performed and overlay images were generated in Photoshop CS (version 8.0, Adobe Systems, San Jose, CA). NeuroLucida software (version 4.36, MicroBrightField, Inc., Williston, VT) was used to follow cell profiles through serial optical sections.

Reagents

Reagents were obtained from Sigma Chemical (St. Louis, MO), sources listed previously (Partida et al., 2004), or the following: Aldrich Chemical (Milwaukee, WI): Li_2CO_3 (#25,582-3); GIBCO (Grand Island, NY): Hank's balanced salt solution (#24020); Invitrogen (Carlsbad, CA): Benchmark (#10747-012), NuPage LDS sample buffer (#NP0007), NuPage Reducing agent (#NP0004), See Blue (#LC5925); Matheson, Coleman, and Bell (Norwood, OH): picric acid (#PX1165); Molecular Probes (Eugene, OR): 10 kD dextran coupled to Alexa Fluor 568 (#D22912), Image-iT FX Signal Enhancer (#I36933); Reckitt Benckiser Pharmaceuticals (Richmond VA): buprenorphine hydrochloride (#NDC 12496-0757-1); Roche (Indianapolis, IN): beta glycerol phosphate (#G6376), sodium fluoride (#S6521), sodium orthovanadate (#S6508).

Antibodies

We tested anti-HCN4 antisera generated against different amino acid sequences of the HCN4 isoform. One was an affinity-purified rabbit polyclonal IgG against amino acids 119–155 of human HCN4 (Chemicon #AB5808; Temecula, CA). The other was a rat monoclonal against amino acids 1046–1083 of rat HCN4 (Abcam #ab32675; Cambridge, MA). These were used with species-specific secondary antibodies, e.g. donkey anti-rabbit IgG coupled to horseradish peroxidase (Amersham, #NA934V; Piscataway, NJ) for the western blots, and goat anti-rabbit coupled to Alexa Fluor 488 (Molecular Probes, #A11034) for the flat mounts shown. This fluorophore and that coupled to the dextran were selected because their excitation and emission wavelengths produced minimal cross-contamination during our attempts to stain retrogradely labeled ganglion cells (cf. Partida et al., 2004). Tissues incubated in secondary antibodies without any primary antisera displayed no fluorescence at the confocal imaging and display settings used to generate any of the figures.

Negative controls for binding of the polyclonal primary antiserum were performed with a sample of the fusion protein that generated this antiserum (Accession # NP_005468). Pairs of blot lanes were run from a single sample of retinal homogenate, and flat-mounted pieces of retina were prepared from a single eye or from opposite eyes of a single animal. While one of the so-paired samples was incubated in a primary antiserum, the other was incubated in primary antiserum that was pre-incubated with the control antigen for either 6 hours at room temperature or overnight at 4 °C; these paired samples were processed identically at all other stages of each protocol.

Results

This study tests whether mammalian retinal ganglion cells bind antibodies directed against a peptide sequence of channels that pass the mixed-cation current known as I_h. We used rat retina because earlier voltage recordings indicated the presence of I_h in rat optic nerve (Eng et al., 1990) and we have shown that I_h can be activated in some rat retinal ganglion cell somata (Lee and Ishida, 2007). We flat-mounted these retinas to examine the distribution and appearance of immunostained ganglion cells, and because these preparations structurally preserved ganglion cell layer somata and ganglion cell axons better than vertically sectioned material. Rabbit polyclonal anti-HCN4 antiserum (Chemicon #AB9338) bound more clearly to ganglion cell somata profiles and processes than other antisera, including some directed against other HCN isoforms. We have therefore started identifying inwardly rectifying channel isoforms in retinal ganglion cells with this antiserum. Because this antiserum differs from that used in previous studies (Müller et al., 2003; Fyk-Kolodziej and Pourcho, 2007), we first show binding to western blotted membrane fraction protein, and then describe the binding to retrogradely labeled retinal ganglion cells.

HCN4 protein in adult rat retinal homogenates

Anti-HCN4 antiserum bound almost exclusively to a single protein band with an apparent molecular weight around 123±12 kD (mean±SD, n=3; e.g., Fig. 1A, “HCN4”). Binding to this band was undetectably low when the primary antiserum was preincubated with control antigen (Fig. 1A, “+block”), as was binding to a few faint bands of higher apparent molecular weight. The 123-kD band agrees with the molecular weight calculated from the rat HCN4 amino acid sequence (129 kD; see the SwissProt database at http://www.expasy.ch/sprot/sprot-top.html) and the apparent molecular weight of retinal protein bound by a rat monoclonal antibody directed against a different amino acid sequence of HCN4 (Müller et al., 2003).

HCN4-like immunoreactivity in retrogradely-labeled ganglion cells

Figure 1B shows fields within a pair of retinas processed identically except that raw primary antiserum was applied to the "test" retina ("HCN4"), while blocked antiserum was applied to the "control" retina ("+block"). These fields were imaged at the ganglion cell layer (shown in the "dextran" panels by the concomitantly imaged somata filled by retrogradely transported dextran) using identical laser intensity, photomultiplier gain, and pinhole settings, and were then displayed at identical image brightness and contrast settings. The AF488 fluorescence seen in the test retina and not in the control retina is therefore referred to below as HCN4-like, isoform-specific "immunoreactivity".

HCN4-like immunoreactivity crisply outlined somata of various sizes and shapes in the ganglion cell layer (Fig. 1B). These outlines were never partial (e.g., semicircular or broken by large gaps), and while profiles of cells were often found closely abutted to those of adjacent cells (Figs. 1, 2), we never found the profile of one cell crossing over or through the profile of other cells in single optical sections. Similar staining of ganglion cell layer somata was observed in vertical sections with a rat monoclonal antibody (Abcam #ab32675) directed against a different amino acid sequence of the HCN4 isoform (not illustrated). This corroborated the staining in flat mounts with the polyclonal antiserum. However, the monoclonal antibody did not produce a comparably clear staining pattern in whole mounts. All observations presented here on cells in flat mounts are therefore based on preparations stained with the polyclonal antiserum.

To demonstrate the relationship of HCN4-like immunoreactivity and retinal ganglion cells identified by retrograde label, paired images of the HCN4 and dextran (like those in Fig. 1B) were collected at several locations in three retinas. When the pairs were merged (e.g., Figs. 2B, C, D), the HCN4-like immunoreactivity (pseudocolored green) colocalized with dextran fill (pseudocolored red) in two ways. First, some of the HCN4-like immunoreactivity formed round or oblong profiles and these were filled by dextran (except for dark areas that resembled nuclei in terms of relative size and position within the cell profile; e.g., Chen et al., 2004). These structures thus appeared as bright red somatic cytoplasm with a green (or greenish-yellow) outline. Secondly, some HCN4-like immunoreactivity extended like stripes across the imaged fields. The position and width of these stripes were matched by dextran-fill (e.g., Figs. 2B–D), identifying these structures as ganglion cell axon fascicles. In superimposed images where the somata appear as medium- to large-sized red dots circumscribed by a sharp green line, these stripes were yellow in color, due to the addition of red and green pseudocolors (Figs. 2B-D). These stripes varied in width (Figs. 2B–D), as do optic fiber layer axon fascicles viewed by other methods (e.g., Peichl, 1989; Huang et al., 2006). No such yellow stripes were seen in retinas if the primary antiserum was preincubated with control antigen.

In addition to the dextran labeling of HCN4-immunopositive axon bundles, some HCN4-like immunoreactivity was sufficiently strong to follow into processes that extended away from individual, dextran-filled somata. These were found to radiate in all directions from somata of at least some cells (e.g., Figs. 1B, 2C), and these included somata of both large and smaller diameters. While these were best resolved as proximal dendrites by their relatively large caliber near somata, some of these could also be followed through serial optical sections as they extended a few tens of micrometers away (not illustrated). However, we saw this too rarely to reconstruct HCN4-immunopositive dendritic arborizations, and as these processes tapered with distance from the somata, the immunoreactivity became too weak to show the extent that dendrites were populated by HCN4 channels.

Distribution of HCN4-immunopositive ganglion cells

Because morphological properties of rodent retinal ganglion cells differ with distance from the optic nerve head (e.g., Dreher et al., 1985), we examined several loci in individual retinas for presence of the staining pattern seen in Fig. 2. For this purpose, we located all of the dextran-backfilled somata and all of the HCN4-immunopositive somata in the ganglion cell layer, in representative locations both near to and far from the optic nerve head, in all four quadrants (nasal, temporal, dorsal and ventral) of three retinas. By doing so (*i*) within 1 mm of the optic nerve head, (*ii*) within 1 mm of the peripheral edge of the retina, and (*iii*) midway between these points, cells were analyzed in a total of twelve loci per retina (e.g., Fig. 2A). Each of the analyzed fields measured ~0.12 mm^2. At each locus, we determined the fraction of dextran-filled ganglion cells that showed HCN4-like immunoreactivity, and measured the size of the HCN4 profile of each cell (including those with and without dextran backfill). Cells were followed through serial optical sections by use of NeuroLucida software (see Methods), and cell size was then determined from the section(s) that circumscribed the full profile of each cell.

Figure 2E shows the distribution of soma diameters for these cells in a single retina, and Table 1 summarizes the data collected from three different retinas. Three results emerged from these measurements. First, the equivalent diameters calculated by averaging the short and long axes of each HCN4-immunopositive, dextran-filled cell ranged from 7 to 30 μm, with an average of 12.7 ± 3 μm (SD; n = 2,818; median 12.0 μm). These values agreed with sizes found in previous anatomical studies of rat retinal ganglion cells (see Huxlin and Goodchild, 1997; Sun et al., 2002). Second, the population density of retrogradely-filled cells in individual fields ranged from 2,468 to 891 cells/mm^2. The highest densities were found within a few mm of the optic disc, in the areas termed “near” and/or “middle” in Table 1. As reported previously for rat retina (Perry, 1981; Danias et al. 2002), these tended to be higher than densities in the periphery. Thus, we counted an average of 1,816 ± 63 dextran-filled cells/mm^2 (mean±SEM) over the 36 fields we imaged, whereas the mean was roughly 2,000 cells/mm^2 when the peripheral fields were not included. These values agree with those identified by retrograde fill with horseradish peroxidase in hooded rats (Perry, 1981), DiI and fast blue in Sprague-Dawley rats (Vidal-Sanz et al., 1988), and FluoroGold in Wistar rats (Danias et al., 2002). Third, approximately 37% of these cells were HCN4-immunopositive. This number varied little across all the retinas we examined (range 32–41 % in 3 retinas) and across all four quadrants in these retinas. Table 1 shows that although the absolute numbers of HCN4-immunopositive ganglion cells differed by as much as 20% between some quadrants (e.g., 568 vs 736 cells per mm^2 in dorsal versus temporal retina, respectively), these comprised a constant fraction of the entire ganglion cell population in each quadrant (due to parallel differences in the total number of ganglion cells). Table 1 also shows that while the ganglion cell density tended to be highest in the central and middle retina and least in the periphery within each quadrant, the HCN4-immunopositive ganglion cell density did not change in parallel. Consequently, the fraction of ganglion cells that are HCN4-immunopositive showed a slight increase (from approximately 32% in the central retinal loci, to 44% in the periphery, and 36% in between).

In addition to the HCN4-immunopositive cells that were dextran-backfilled, an average of 30% of the HCN4-immunopositive cells displayed little or no dextran fill in the fields we analyzed (e.g., Figs. 1, 2). The fraction of the total HCN4-immunopositive cell population that lacked dextran appeared relatively constant from retina to retina, ranging from 25–34% in the three retinas we examined. The number of these cells corresponds to a population density of 289 ± 39 cells/mm^2. The diameter of these somata (calculated by averaging their short and long axes) ranged from 6 to 25 μm, with a mean of 12.5 ± 3 μm (SD; n = 1,248; median 11.9 μm). While these cells seemed slightly smaller than back-filled cells in some fields, we also observed some large somata that were HCN-immunopositive and lacked

retrograde label (e.g., Fig. 2C). Because both ganglion and displaced amacrine cells possess somata in this size range (e.g., Bunt et al., 1974; Perry 1981; Yeh and Olschowka 1989; Larsen et al., 1990; Martin-Martinelli et al., 1994), and because the focus of this study was to test whether dextran-filled cells were HCN4-immunopositive, cells lacking dextran fill remain to be identified.

Discussion

This study provides the first anatomical evidence for presence of the HCN4 channel isoform in somata and processes identified by retrograde labeling as belonging to mammalian retinal ganglion cells. From our observations, one would expect that HCN channels can activate in the axons, somata, and dendrites of some ganglion cells, and that the amplitude and gating kinetics of I_h in these cells might be modulated by intracellular levels of cAMP.

Distribution of HCN channels within single ganglion cells

A basic observation of this study is that anti-HCN4 antiserum binds to membrane fraction protein and to outlines of ganglion cell layer somata, and that binding to both are blocked by the fusion protein that generated the primary antibody. These results would be expected if HCN4 channels are present in rat retinal ganglion cell membranes, and they are consistent with our recordings of I_h in retinal ganglion cell somata (Lee and Ishida, 2007). Similarly, the block of anti-HCN4 antiserum binding to optic fiber layer axon fascicles by control antigen is consistent with the I_h-like voltage rectification in optic nerve (Eng et al., 1990). At the same time, we do not conclude that the somatic and/or axonal conductances are due solely to HCN4 channels, as we have also found HCN1-like immunoreactivity in dextran-labeled somata and optic fiber layer axon fascicles (unpublished observations). This is consistent with the finding of HCN1-like immunoreactivity in retinal ganglion cell layer somata by three previous studies (Kim et al., 2003; Müller et al., 2003; Fyk-Kolodziej and Pourcho, 2007). However, we neither mapped HCN1-i mmunopositive cells in detail, nor compared the binding of anti-HCN1 and anti-HCN4 antisera, because the staining with the former was not as clear as the latter.

Presence of HCN channels in some ganglion and amacrine cells

The HCN4-like immunoreactivity we found seems indiscriminate in one respect, and yet specific in another. To begin with, we found this immunoreactivity in dextran-filled somata having diameters as small as 7 and as large as 30 μm. This spans the range of ganglion cell soma diameters found by other methods in rat retina (Huxlin and Goodchild, 1997; Sun et al., 2002), indicating that HCN4 channels should be available for activation in ganglion cells having small, medium, and large somata. This is interesting, in part, because the largest diameters are typically attributed to α-type ganglion cells, and yet inward rectification was not found in recordings from somata of such large cells, either in rat (Reiff and Guenther, 1999) or cat (O'Brien et al., 2002). These results raise the possibility that HCN4 channels are present in large non-α ganglion cells (e.g., the δ type identified by Peichl, 1989; see also Huxlin and Goodchild, 1997; Sun et al., 2002) and/or that properties of I_h in α-cells render it difficult to detect.

At the same time, we found HCN4-like immunoreactivity in nearly half of the ganglion cells that we were able to back-fill by fluorophore-coupled dextran. This is not altogether surprising, because patch-clamp recording has indicated that some, but not all, morphologically identified subtypes of ganglion cell in cat retina possess a hyperpolarization-activated, slowly gating, inwardly rectifying, and thus HCN-like, conductance (O'Brien et al., 2002). More recently, we found that the current passing through this type of conductance can be activated in some, but not all, rat retinal ganglion cells (Lee

and Ishida, 2007). The images we present here substantiate these results because we found a similar fraction of HCN4-to-dextran cells in all of the fields we examined in 3 well-stained retinas. However, until we can show which of the morphological subtypes of ganglion cell in rat retina (Huxlin and Goodchild, 1997; Sun et al., 2002) display HCN4-like immunoreactivity, we would not attempt to account for our having found HCN4-like immunoreactivity in some small, medium, and large somata, and not in others.

We know of no method that guarantees staining all of the ganglion cells in a given retina. Thus, in preparations identifying dextran-filled cells as ganglion cells, one might not be able to identify a small number of cells in the ganglion cell layer that lacked dextran fills as displaced amacrine cells. On the other hand, the numbers of dextran-filled cells in the preparations we analyzed agreed with ganglion cell densities identified by other methods (Perry, 1981; Vidal-Sanz et al., 1988; Danias et al., 2002). Thus, the fairly numerous ganglion cell layer somata we found with HCN4-like immunoreactivity and no dextran backfill may be displaced amacrine cells. If these were ganglion cells that bound anti-HCN4 antibody and failed to fill with dextran, one might expect the density of our filled cells to be at least 30% fewer than ganglion cell densities reported by other studies.

Two previous studies applied anti-HCN4 antisera to western blots and vertical sections prepared from rat retina (Müller et al., 2003; Fyk-Kolodziej and Pourcho, 2007). The western blots resemble ours in showing that anti-HCN4 antisera (rat monoclonal and rabbit polyclonal) bind to a protein band with an estimated molecular weight of 132–155 kD. Likewise, a few immunopositive ganglion cell layer somata can be seen in Figures 2B, 3A, and 3F of the first study (Müller et al., 2003). In fact, after commenting on immunoreactivity in the inner plexiform layer, this study stated that “Few amacrine cells and somata in the GCL were also immunoreactive”. The latter observation is at least qualitatively similar to ours. The more recent study (Fyk-Kolodziej and Pourcho, 2007) did not mention finding HCN4 immunoreactivity in ganglion cell layer somata. While this appears to differ from both our observations and those of Muller et al. (2003), it remains unclear whether this is a meaningful difference.

Presence of cAMP-sensitive channels in ganglion cells

The presence of a slowly gating, inwardly rectifying conductance in some ganglion cells and not in others (Reiff and Guenther, 1999; O’Brien et al., 2002; Chen et al. 2004; Lee and Ishida, 2007) is consistent with the possibility that HCN channels contribute to light responses of particular cells. In this respect, HCN4 channels are interesting to investigate because their voltage sensitivity is altered to a greater extent by cAMP than in any of the other mammalian HCN isoforms (e.g., Ludwig et al., 1998; Santoro et al., 2000). This would predict that the contribution of I_h to resting membrane potential and resistance (Lee and Ishida, 2007) and to rebound excitation (Tabata and Ishida, 1996; Lee et al., 2003; Lee and Ishida, 2007) is increased by conditions that elevate intracellular cAMP levels (Vaquero et al., 2001; Nir et al., 2002; Dunn et al., 2006; Mills et al. 2007). However, properties of the net current are shaped by the presence of other HCN isoforms (Franz et al., 2000; Santoro et al., 2000; Altomare et al., 2001; Chen et al., 2001). It would therefore be natural for future studies to test the possibility that HCN4 channels co-localize with other HCN channels in retinal ganglion cells.

Acknowledgments

This work was supported by grants from the National Eye Institute of the NIH (EY 08120 and P30 EY12576), as well as from Research to Prevent Blindness. We thank L.M. Hjelmeland and P.G. FitzGerald for advice on fixation via cardiac perfusion, L.M. Chalupa and D. van der List for use of NeuroLucida software, E.G. Jones and A. Graziano for use of a Nikon Eclipse E1000 microscope, and T. Tan for participation in some of the blotting experiments.

References

Altomare C, Bucchi A, Camatini E, Baruscotti M, Viscomi C, Moroni A, DiFrancesco D. Integrated allosteric model of voltage gating of HCN channels. Journal of General Physiology. 2001; 117:519–532. [PubMed: 11382803]

Bunt AH, Lund RD, Lund JS. Retrograde axonal transport of horseradish peroxidase by ganglion cells of the albino rat retina. Brain Research. 1974; 73:215–228. [PubMed: 4133900]

Chen L, Yu YC, Zhao JW, Yang XL. Inwardly rectifying potassium channels in rat retinal ganglion cells. European Journal of Neuroscience. 2004; 20:956–964. [PubMed: 15305864]

Chen S, Wang J, Siegelbaum SA. Properties of hyperpolarization-activated pacemaker current defined by coassembly of HCN1 and HCN2 subunits and basal modulation by cyclic nucleotide. Journal of General Physiology. 2001; 117:491–504. [PubMed: 11331358]

Danias J, Shen F, Goldblum D, Chen B, Ramos-Esteban J, Podos SM, Mittag T. Cytoarchitecture of the retinal ganglion cells in the rat. Investigative Ophthalmology and Visual Science. 2002; 43:587–594. [PubMed: 11867571]

Dreher B, Sefton AJ, Ni SY, Nisbett G. The morphology, number, distribution and central projections of Class I retinal ganglion cells in albino and hooded rats. Brain, Behavior and Evolution. 1985; 26:10–48.

Dunn TA, Wang CT, Colicos MA, Zaccolo M, DiPilato LM, Zhang J, Tsien RY, Feller MB. Imaging of cAMP levels and protein kinase A activity reveals that retinal waves drive oscillations in second-messenger cascades. Journal of Neuroscience. 2006; 26:12807–12815. [PubMed: 17151284]

Eng DL, Gordon TR, Kocsis JD, Waxman SG. Current-clamp analysis of a time-dependent rectification in rat optic nerve. Journal of Physiology. 1990; 421:185–202. [PubMed: 2348391]

Franz O, Liss B, Neu A, Roeper J. Single-cell mRNA expression of HCN1 correlate with a fast gating phenotype of hyperpolarization-activated cyclic nucleotide-activated ion channels (Ih) in central neurons. European Journal of Neuroscience. 2000; 12:2685–2693. [PubMed: 10971612]

Fyk-Kolodziej B, Pourcho RG. Differential distribution of hyperpolarization-activated and cyclic nucleotide-gated channels in cone bipolar cells of the rat retina. Journal of Comparative Neurology. 2007; 501:891–903. [PubMed: 17311321]

Hayashida Y, Ishida AT. Dopamine receptor activation can reduce voltage-gated Na^+ current by modulating both entry into and recovery from inactivation. Journal of Neurophysiology. 2004; 92:3134–3141. [PubMed: 15486428]

Huang XR, Knighton RW, Shestopalov V. Quantifying retinal nerve fiber layer thickness in whole-mounted retina. Experimental Eye Research. 2006; 83:1096–1101. [PubMed: 16828473]

Huxlin KR, Goodchild AK. Retinal ganglion cells in the albino rat: revised morphological classification. Journal of Comparative Neurology. 1997; 385:309–323. [PubMed: 9268130]

Kim IB, Lee EJ, Kang TH, Chung JW, Chun MH. Morphological analysis of the hyperpolarization-activated cyclic nucleotide-gated cation channel 1 (HCN1) immunoreactive bipolar cells in the rabbit retina. Journal of Comparative Neurology. 2003; 467:389–402. [PubMed: 14608601]

Kim KJ, Rieke F. Temporal contrast adaptation in the input and output signals of salamander retinal ganglion cells. Journal of Neuroscience. 2001; 21:287–299. [PubMed: 11150346]

Koizumi A, Jakobs TC, Masland RH. Inward rectifying currents stabilize the membrane potential in dendrites of mouse amacrine cells: patch-clamp recordings and single-cell RT-PCR. Molecular Vision. 2004; 10:328–340. [PubMed: 15152185]

Larsen JN, Bersani M, Olcese J, Holst JJ, Møller M. Somatostatin and prosomatostatin in the retina of the rat: an immunohistochemical, in-situ hybridization, and chromatographic study. Visual Neuroscience. 1990; 5:441–452. [PubMed: 1981146]

Lee SC, Hayashida Y, Ishida AT. Availability of low-threshold Ca^{2+} current in retinal ganglion cells. Journal of Neurophysiology. 2003; 90:3888–3901. [PubMed: 14665686]

Lee SC, Ishida AT. I_h without K_{ir} in adult rat retinal ganglion cells. Journal of Neurophysiology. 2007; 97:3790–3799. [PubMed: 17488978]

Lipton SA, Tauck DL. Voltage-dependent conductances of solitary ganglion cells dissociated from the rat retina. Journal of Physiology. 1987; 385:361–391. [PubMed: 2443669]

Ludwig A, Zong X, Jeglitsch M, Hofmann F, Biel M. A family of hyperpolarization-activated mammalian cation channels. Nature. 1998; 393:587–591. [PubMed: 9634236]

Lukasiewicz PD, Werblin FS. A slowly inactivating potassium current truncates spike activity in ganglion cells of the tiger salamander retina. Journal of Neuroscience. 1988; 8:4470–4481. [PubMed: 3199187]

Martin-Martinelli E, Savy C, Nguyen-Legros J. Morphometry and distribution of displaced dopaminergic cells in rat retina. Brain Research Bulletin. 1994; 34:467–482. [PubMed: 8082039]

Mills SL, Xia XB, Hoshi H, Firth SI, Rice ME, Frishman LJ, Marshak DW. Dopaminergic modulation of tracer coupling in a ganglion-amacrine cell network. Visual Neuroscience. 2007; 24:1–16. [PubMed: 17430604]

Moosmang S, Stieber J, Zong X, Biel M, Hofmann F, Ludwig A. Cellular expression and functional characterization of four hyperpolarization-activated pacemaker channels in cardiac and neuronal tissues. European Journal of Biochemistry. 2001; 268:1646–1652. [PubMed: 11248683]

Müller F, Scholten A, Ivanova E, Haverkamp S, Kremmer E, Kaupp UB. HCN channels are expressed differentially in retinal bipolar cells and concentrated at synaptic terminals. European Journal of Neuroscience. 2003; 17:2084–2096. [PubMed: 12786975]

Nir I, Harrison JM, Haque R, Low MJ, Grandy DK, Rubinstein M, Iuvone PM. Dysfunctional light-evoked regulation of cAMP in photoreceptors and abnormal retinal adaptation in mice lacking dopamine D4 receptors. Journal of Neuroscience. 2002; 22:2063–2073. [PubMed: 11896146]

O'Brien BJ, Isayama T, Richardson R, Berson DM. Intrinsic physiological properties of cat retinal ganglion cells. Journal of Physiology. 2002; 538:787–802. [PubMed: 11826165]

Partida GJ, Lee SC, Haft-Candell L, Nichols GS, Ishida AT. DARPP-32-like immunoreactivity in AII amacrine cells of rat retina. Journal of Comparative Neurology. 2004; 480:251–263. [PubMed: 15515184]

Peichl L. Alpha and delta ganglion cells in the rat retina. Journal of Comparative Neurology. 1989; 286:120–139. [PubMed: 2768556]

Perry VH. Evidence for an amacrine cell system in the ganglion cell layer of the rat retina. Neuroscience. 1981; 6:931–944. [PubMed: 6165929]

Reiff DF, Guenther E. Developmental changes in voltage-activated potassium currents of rat retinal ganglion cells. Neuroscience. 1999; 92:1103–1117. [PubMed: 10426549]

Santoro B, Tibbs GR. The HCN gene family: molecular basis of the hyperpolarization-activated pacemaker channels. Annals of the New York Academy of Sciences. 1999; 868:741–764. [PubMed: 10414361]

Santoro B, Chen S, Luthi A, Pavlidis P, Shumyatsky GP, Tibbs GR, Siegelbaum SA. Molecular and functional heterogeneity of hyperpolarization-activated pacemaker channels in the mouse CNS. Journal of Neuroscience. 2000; 20:5264–5275. [PubMed: 10884310]

Sun W, Li N, He S. Large-scale morphological survey of rat retinal ganglion cells. Visual Neuroscience. 2002; 19:483–493. [PubMed: 12511081]

Tabata T, Ishida AT. Transient and sustained depolarization of retinal ganglion cells by I_h. Journal of Neurophysiology. 1996; 75:1932–1943. [PubMed: 8734592]

Vaquero CF, Pignatelli A, Partida GJ, Ishida AT. A dopamine- and protein kinase A-dependent mechanism for network adaptation in retinal ganglion cells. Journal of Neuroscience. 2001; 21:8624–8635. [PubMed: 11606650]

Vidal-Sanz M, Villegas-Perez MP, Bray GM, Aguayo AJ. Persistent retrograde labeling of adult rat retinal with the carbocyanine dye dil. Experimental Neurology. 1988; 102:92–101. [PubMed: 3181354]

Yeh HH, Olschowka JA. A system of corticotropin releasing factor-containing amacrine cells in the rat retina. Neuroscience. 1989; 33:229–240. [PubMed: 2601858]

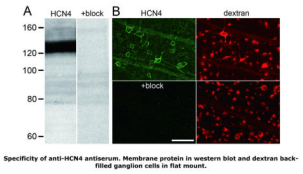

FIGURE 1.

Specificity of anti-HCN4 antiserum binding. **A**: Western blots of retinal membrane fraction proteins, identically prepared and formatted, except that the lane labeled “HCN4” was probed with anti-HCN4 antibody, while the lane labeled “+block” was incubated in anti-HCN4 antibody pre-incubated with control antigen. Tick marks show distance migrated in neighboring lanes by protein standards of the molecular weights indicated (in kD). The anti-HCN4 antiserum bound specifically to a band at 123 kD. **B**: Ganglion cell layer somata and optic fiber layer axon fascicles in two flat-mounted retinas, processed and imaged identically, except that one retina (“HCN4”) was incubated in anti-HCN4 antibody, while the other (“+block”) was incubated in anti-HCN4 antibody pre-incubated with control antigen. The ganglion cells in each retina were filled by fluorophore-coupled dextran introduced into the optic nerve, so that HCN4-like immunoreactivity (i.e., Alexa Fluor 488 fluorescence) could be imaged while focusing on the ganglion cell somata. Comparison of the “HCN4” and “+block” fields shows that control antigen blocked anti-HCN4 antibody binding. Comparison of the “HCN4” and corresponding dextran fields shows that HCN4-like immunoreactivity circumscribed ganglion cell somata and tracked axon fascicles extending across the field (between the upper left and lower right). Each image is a single confocal optical section collected with a 40x oil immersion objective. Scale bar is 50 μm and applies to all panels.

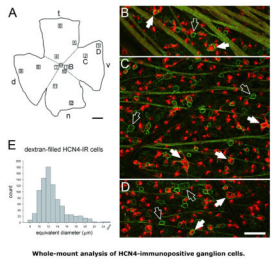

FIGURE 2.

Distribution of HCN4-immunopositive ganglion cells. **A**: Outline of flat-mounted retina, immunostained for HCN4 after ganglion cells were dextran-backfilled. Optic nerve head labeled “ON”. Dorsal, temporal, ventral, and nasal sides of retina labeled “d”, “t”, “v” and “n”, respectively. Scale bar is 1 mm. **B**, **C**, **D**: Panels superimposing the AF488 fluorescence (HCN4-like immunoreactivity, pseudocolored green) and AF568 fluorescence (the dextran-coupled fluorophore, pseudocolored red) of a field near the optic disc (**B**), the mid-periphery (**C**), and the far periphery (**D**). The positions of these fields are shown by the corresponding letters in **A**. Ganglion cell somata appear red, with and without green outlines. Filled arrows point to HCN4-immunopositive, dextran-filled somata; empty arrows point to HCN4-immunopositive somata lacking dextran-fill. Striped-shaped fascicles of intraretinal ganglion cell axons appear greenish yellow. HCN4-like immunoreactivity also outlines thick proximal dendrites, e.g., those of the large soma at the lower edge of panel **C**. The dark tubular structures extending across panels **B**, **C**, and **D** are blood vessels that were perfused with Hank’s solution prior to fixation. Scale bar is 50 μm for all fields. **E**: Histogram of HCN4-immunopositive ganglion cell somata diameters in the 12 areas numbered in **A**. Diameters are average of short and long axis. Central (1, 4, 7, 10), mid-peripheral (2, 5, 8, 11), and far-peripheral (3, 6, 9, 12) fields were imaged in each retinal quadrant (dorsal, ventral, temporal, and nasal).

Table 1

Density of HCN4-immunopositive retinal ganglion cells at twelve loci across surface of three retinas.

quadrant	location relative to optic nerve disc	dextran-filled cells	HCN4-positive dextran-filled cells		
		local density (cells/mm^2 ± SEM; n=3 fields)	local density (n=3 fields)	quadrant average (n=9 fields)	percent of dextran-filled cells
dorsal	near	1890 (± 107)	569 (± 72)	568 (± 52)	37
	middle	1543 (± 221)	568 (± 104)		
	peripheral	1170 (± 166)	565 (± 128)		
ventral	near	2098 (± 144)	614 (± 51)	703 (± 49)	37
	middle	2003 (± 49)	781 (± 138)		
	peripheral	1617 (± 181)	715 (± 12)		
nasal	near	1961 (± 151)	652 (± 22)	619 (± 34)	32
	middle	2036 (± 42)	698 (± 41)		
	peripheral	1772 (± 148)	508 (± 48)		
temporal	near	2097 (± 220)	678 (± 68)	736 (± 56)	37
	middle	2128 (± 240)	639 (± 99)		
	peripheral	1721 (± 303)	891 (± 74)		